

Title:

Enhancing HMMWV Operational Availability through the use of an Instrumented Diagnostic Cleat for Condition-Based Maintenance

Authors:

Tiffany DiPetta, Douglas E. Adams¹

Joseph Gotham, Paul Decker, James Bechtel, David Lamb, Ph.D., David Gorsich,
Ph.D.²

Grant A. Gordon³

George L. Wright⁴

¹ Purdue University, 1500 Kepner Drive, Lafayette, IN 47905

² Tank Automotive Research, Development and Engineering Center, Warren, MI

³ Honeywell Aerospace, 111 S. 34th St. M/S 503-121, Phoenix, AZ 85034

⁴ Honeywell Defense & Space, 9201 San Mateo Blvd., NE M/S B6, Albuquerque,
NM 87113-2227

Report Documentation Page			Form Approved OMB No. 0704-0188		
<p>Public reporting burden for the collection of information is estimated to average 1 hour per response, including the time for reviewing instructions, searching existing data sources, gathering and maintaining the data needed, and completing and reviewing the collection of information. Send comments regarding this burden estimate or any other aspect of this collection of information, including suggestions for reducing this burden, to Washington Headquarters Services, Directorate for Information Operations and Reports, 1215 Jefferson Davis Highway, Suite 1204, Arlington VA 22202-4302. Respondents should be aware that notwithstanding any other provision of law, no person shall be subject to a penalty for failing to comply with a collection of information if it does not display a currently valid OMB control number.</p>					
1. REPORT DATE 04 JUL 2009	2. REPORT TYPE Journal Article	3. DATES COVERED 07-03-2008 to 10-06-2009			
4. TITLE AND SUBTITLE Enhancing HMMWV Operational Availability through the use of an Instrumented Diagnostic Cleat for Condition-Based Maintenance			5a. CONTRACT NUMBER W911NF-07-D-0001		
			5b. GRANT NUMBER		
			5c. PROGRAM ELEMENT NUMBER		
6. AUTHOR(S) Tiffany DiPetta; Douglas Adams; Joseph Gotham; Paul Decker; David Gorsich			5d. PROJECT NUMBER		
			5e. TASK NUMBER		
			5f. WORK UNIT NUMBER		
7. PERFORMING ORGANIZATION NAME(S) AND ADDRESS(ES) Purdue University,1500 Kepner Drive,Lafayette,IN,47905			8. PERFORMING ORGANIZATION REPORT NUMBER ; #19904		
9. SPONSORING/MONITORING AGENCY NAME(S) AND ADDRESS(ES) U.S. Army TARDEC, 6501 East Eleven Mile Rd, Warren, Mi, 48397-5000			10. SPONSOR/MONITOR'S ACRONYM(S) TARDEC		
			11. SPONSOR/MONITOR'S REPORT NUMBER(S) #19904		
12. DISTRIBUTION/AVAILABILITY STATEMENT Approved for public release; distribution unlimited					
13. SUPPLEMENTARY NOTES Suhbmitted to the 2009 International Workshop on Structural Health Monitoring					
14. ABSTRACT A rubber cleat is instrumented with two triaxial accelerometers to measure the multi-directional response of the cleat due to the forces within the tire footprint of a ground vehicle. The cleat data is used to detect faults in the front and rear suspension in addition to the wheel tire despite variability in the data. This offboard diagnostic technique is proposed to enable condition-based maintenance.					
15. SUBJECT TERMS					
16. SECURITY CLASSIFICATION OF:			17. LIMITATION OF ABSTRACT	18. NUMBER OF PAGES	19a. NAME OF RESPONSIBLE PERSON
a. REPORT unclassified	b. ABSTRACT unclassified	c. THIS PAGE unclassified	Public Release	10	

ABSTRACT

A rubber cleat is instrumented with two triaxial accelerometers to measure the multi-directional response of the cleat due to the forces within the tire footprint of a ground vehicle. The cleat data is used to detect faults in the front and rear suspension in addition to the wheel tire despite variability in the data. This offboard diagnostic technique is proposed to enable condition-based maintenance.

INTRODUCTION

The U.S. Army is pursuing health monitoring technologies that will enable Condition Based Maintenance (CBM) for military wheel vehicles such as the High Mobility Multipurpose Wheeled Vehicle (HMMWV). The most common faults in the HMMWV occur in the wheel ends, suspension, and frame (Thomas, 1985). Vehicle health monitoring is conventionally performed using onboard measurement and analysis systems. Two principle difficulties exist with onboard systems. First, onboard systems require that sensors and data acquisition hardware be installed on every vehicle. Second, vehicles are subjected to a wide range of terrains and operating conditions. As a result, the number of datasets required to characterize the possible healthy signatures for an N -dimensional vehicle sensor suite, considering M operational terrains, is on the order M^N . The prohibitive amount of data that would be required for fault identification motivated our interest in augmenting onboard health management systems with an off-board health monitoring approach.

The instrumented diagnostic cleat was developed to overcome the economic and technical barriers associated with onboard health monitoring systems. The diagnostic cleat measures the dynamic response of the vehicle as it traverses the cleat at a fixed speed. Then the dynamic response is compared to a reference (or healthy) response to detect anomalies, which correspond to faults within the vehicle. The diagnostic cleat eliminates the technical challenges associated with variations in the terrain assuming a fixed vehicle speed and cleat profile. The cleat also eliminates the need for onboard vehicle equipment and it is portable so one cleat can diagnose a fleet of vehicles. An analytical study of the diagnostic cleat for fault

identification was conducted in DiPetta et al. (2009), and experiments on a HMMWV are described in this paper.

ANALYSIS

Experimental Setup and Procedure

The experiment was conducted with a rubber cleat, which was instrumented with two tri-axial accelerometers (Fig. 1(a)). The accelerometers were installed on the medium plane of the cleat on the left and right sides so that the measured accelerations would be sensitive to the left and right tire forces exerted by a HMMWV traversing the cleat. The HMMWV was driven over the cleat multiple times in the East and West bound directions at 5 mph for each set of tests (Fig. 1(b)).

The experiment consisted of five tests: two baselines (initial and final), two simulated suspension faults, and one simulated tire fault. The final baseline test was conducted after all other tests had been completed. The baseline condition consisted of front tire pressures of 20 psi and rear tire pressures of 22 psi. The two suspension faults were simulated by inserting a metal wedge into the front-right and rear left suspension coil springs. The tire pressure test was conducted by reducing the tire pressure in the front-right tire to 14 psi.

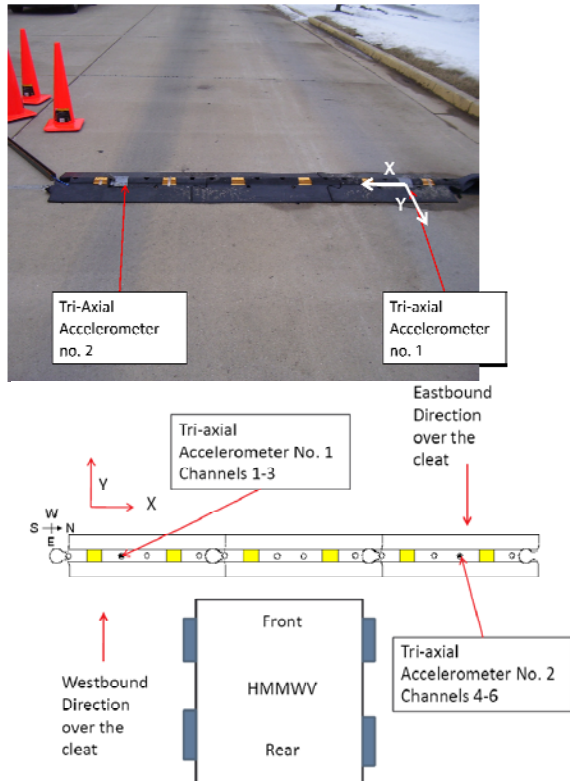


Figure 1: (a) Instrumented cleat, and (b) test configuration.

Experimental Results

Figure 2 shows the acceleration measurements in the X, Y, and Z directions for accelerometers #1 and #2. The acceleration amplitudes are within $\pm 5g$ ($1 g = 9.81 \text{ m/s}^2$). Peak levels from both accelerometers are comparable in the X, Y, and Z directions. Two main events are evident in the time histories corresponding to when the vehicle enters and exits the cleat. When the vehicle enters the cleat, the largest acceleration amplitudes occur in the Y (vehicle movement/tracking) and Z (vertical) directions due to the forward momentum of the vehicle and the vertical profile of the cleat. The lowest amplitude accelerations occur in the lateral direction (along axis of the cleat). There is a small delay between the left and right accelerometer responses due to the cleat's orientation relative to the oncoming vehicle direction. The direction can be determined based on this small delay as described below. If the length between the front and rear wheels is known, the speed of a vehicle can be determined by observing the delay between the front wheel crossing and the rear wheel crossing.

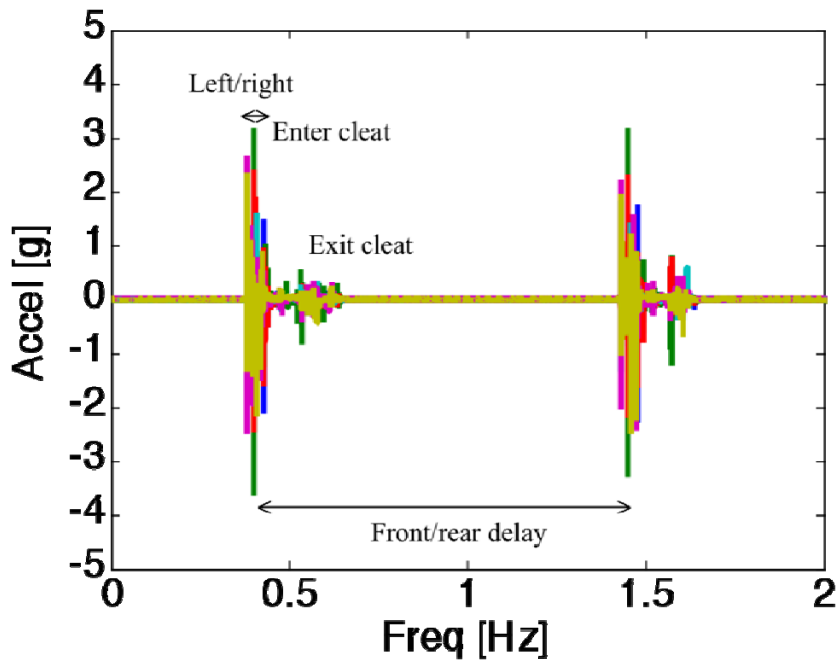


Figure 2: Time histories spectra for initial baseline (East bound) with three channels of acceleration data in the X, Y, and Z directions on both sides of the instrumented cleat (vehicle moving East bound, right side: (—) X, (—) Y, and (—) Z; and left side: (—) X, (—) Y, and (—) Z).

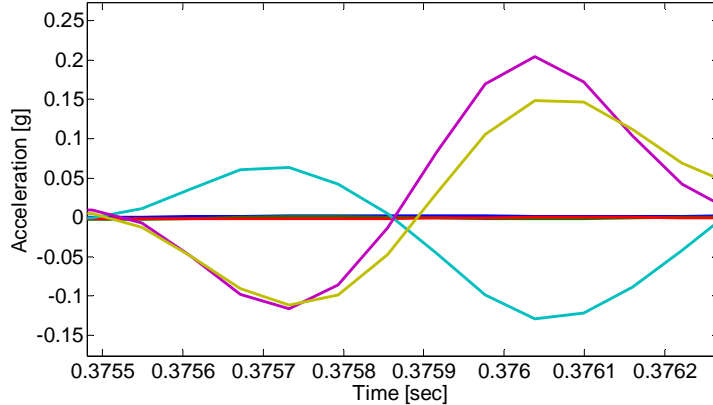


Figure 3: (—) X, (—) Y, and (—) Z accelerations for accelerometer #2 for East bound traveling vehicle over the cleat (front wheels).

Accelerometer #2 is the first to register a response as the vehicle travels in the East bound direction over the cleat. The average data acquired across 10 tests for the X, Y, and Z directions of acceleration are plotted in Figure 3 as the left-front tire begins to traverse the cleat. This data indicates that the Y and Z accelerations are in phase whereas the X acceleration is out of phase with the other two channels as the front left tire travels over the cleat. This behavior is expected based on the forces exerted by the wheel on the cleat. Specifically, the wheel exerts an outward lateral force (+X) on the cleat in addition to a forward tracking force (-Y) and downward vertical force (-Z). The data indicates that there is very little response in accelerometer #1 in this portion of the measurement. This result suggests that there is negligible coupling, or cross-talk, between the two sensors installed within the cleat for this particular measurement. From a data analysis point of view, this low amount of coupling between the two sensorized segments of the instrumented cleat dataset is critical to enable diagnosis of fault conditions (left or right wheel).

As the vehicle continues to move forward, accelerometer #1 registers its transient response as shown in Figure 4. The X, Y, and Z directions of acceleration indicate that all three channels are in phase as the right-front wheel traverses the cleat. This behavior is expected based on the same logic that was used above to interpret the data taken using accelerometer #2. Namely, the right front wheel pushes laterally outward (-X) on the cleat, forward (-Y) in the direction of vehicle travel, and downward (-Z). All of these dynamic forces produce negative accelerations in the measured data that is acquired using accelerometer #1. As in the previous set of acceleration measurements, there appears to be very little coupling between this measurement of the dynamic response of the cleat due to the forces exerted by the right-front wheel at accelerometer #1 and the measurement at the other side of the cleat in the proximity of accelerometer #2.

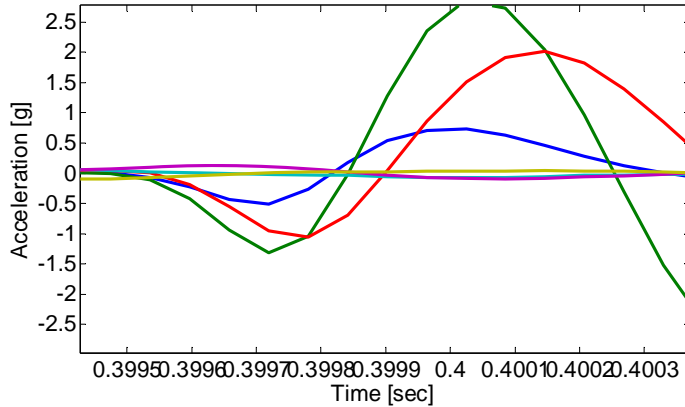


Figure 4: (—) X, (—) Y, and (—) Z accelerations for accelerometer #1 for East bound traveling vehicle over the cleat (front wheels).

These two results taken together suggest that the direction of travel of the vehicle can be determined if the vehicle approach direction is not perpendicular to the line between accelerometers #1 and #2. This ability to determine the direction of travel could be important from an operational perspective. For instance, a vehicle traveling out of the depot could be distinguished from one that is traveling into the depot for service and maintenance using only one cleat based on this approach.

Figure 5 shows the spectra of the acceleration measurements for the two accelerometers in the initial baseline condition of the vehicle for data that was acquired when only the front wheels traversed the cleat. The largest amplitudes are again exhibited in the two Y and Z direction measurements, whereas the smallest amplitudes are exhibited in the two X direction measurements. The Z direction response for accelerometer #2 is particularly large over the frequency range below 500 Hz. There is clustering in the measured response spectra in certain frequency range below 100 Hz, near 250 and 750 Hz, and again near 1200 Hz. The low frequency response is dominated by global suspension (sprung) and wheel (unsprung) dynamic behavior whereas the higher frequency response amplitudes are dominated by local dynamic behavior in the tire and suspension components.

Figure 6 shows a comparison of the frequency spectra between 0 and 100 Hz for the initial baseline, final baseline, right-front suspension coil fault, and right-front tire pressure fault datasets. The six spectra correspond to the three X, Y, and Z accelerations for accelerometers #1 and #2. Note that the Z direction acceleration response for accelerometer #2 is largest over the entire frequency range and the Y direction acceleration response for accelerometer #2 is second largest as observed in Figure 5. Due to these significant differences in the amplitudes of response measured by accelerometers #1 and #2 for an East bound vehicle motion over the cleat, the frequency response functions of the cleat were further analyzed by considering datasets that were acquired for the East bound and West bound motions.

UNCLAS: Dist A. Approved for public release

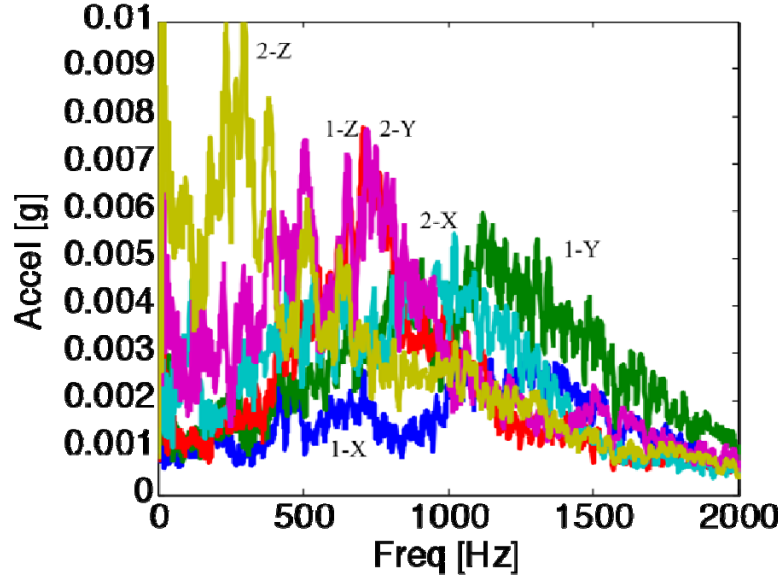


Figure 5: Frequency spectra for initial baseline (East bound) with three channels of acceleration data in the X, Y, and Z directions on both sides of the instrumented cleat (Looking East bound, right side: (—) X, (—) Y, and (—) Z; and left side: (—) X, (—) Y, and (—) Z).

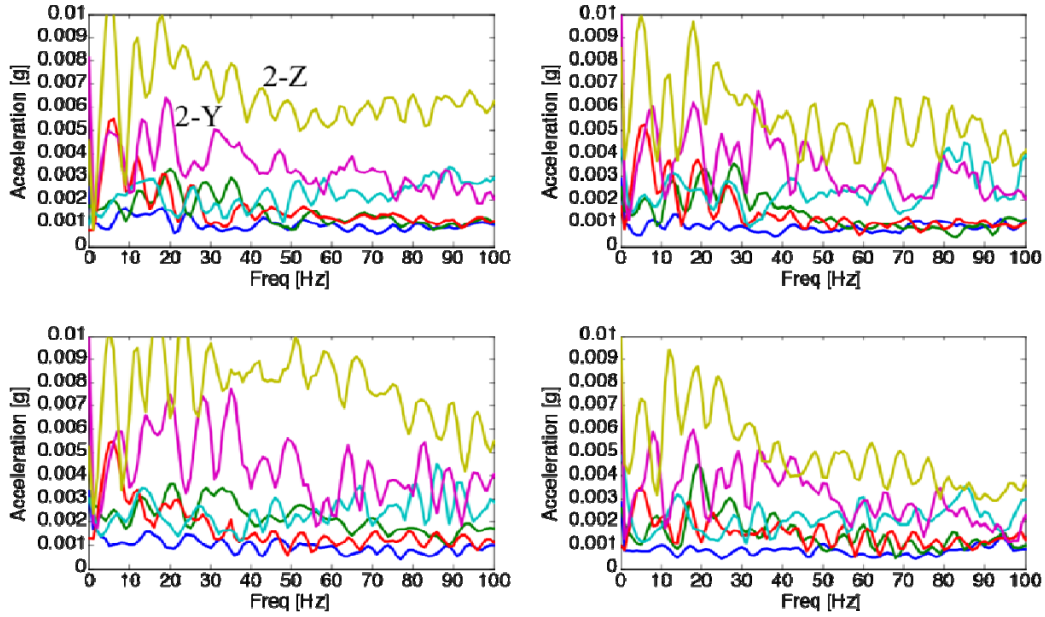


Figure 6: Frequency spectra for (a) initial baseline, (b) final baseline, (c) right-front suspension fault, and (d) right-front tire pressure fault with three channels of acceleration data in the X, Y, and Z directions on both sides of the instrumented cleat (right side: (—) X, (—) Y, and (—) Z; and left side : (—) X, (—) Y, and (—) Z).

The frequency response function relating a force in the left wheel to the response of accelerometer #2 is denoted by $H_2(\omega)$, and the corresponding frequency response function for the right wheel near accelerometer #1 is denoted by $H_1(\omega)$. It is assumed that the frequency response functions that relate input forces from the tire footprint to output acceleration responses in the cleat are equal for the vehicle

traveling in the East and West bound directions. Given these assumptions, the equations relating the measured accelerations $A_{1e}(\omega)$ and $A_{2e}(\omega)$ for East bound travel and $A_{1w}(\omega)$ and $A_{2w}(\omega)$ for West bound travel are given by:

$$\begin{aligned} A_{1e}(\omega) &= H_1(\omega)F_R(\omega) \\ A_{2e}(\omega) &= H_2(\omega)F_L(\omega) \\ A_{1w}(\omega) &= H_1(\omega)F_L(\omega) \\ A_{2w}(\omega) &= H_2(\omega)F_R(\omega) \end{aligned} \quad (1a,b,c,d)$$

Therefore, the following relationships between the frequency response functions and forces that were estimated on the right and left hand sides of the cleat can be derived:

$$\begin{aligned} \frac{A_{1e}(\omega) + A_{1w}(\omega)}{A_{2e}(\omega) + A_{2w}(\omega)} &= \frac{H_1(\omega)}{H_2(\omega)} \\ \frac{A_{1e}(\omega) + A_{2w}(\omega)}{A_{2e}(\omega) + A_{1w}(\omega)} &= \frac{F_R(\omega)}{F_L(\omega)} \end{aligned} \quad (2a,b)$$

These formulae were used to calculate and plot the ratios for the left and right hand sides of the cleat to develop insight about the cleat and vehicle symmetry. The initial baseline data for East and West bound directions were used.

Figure 7 shows the magnitudes of the (a) frequency response and (b) force ratios as a function of frequency based on the formulae in Eq. (2). The three curves correspond to the ratios for the X, Y, and Z direction measurements. The upper plot indicates that the Z direction response for accelerometer #1 is attenuated relative to the Z direction response for accelerometer #2 in the low frequency range below 100 Hz (see expanded frequency range). This result is consistent with the data in Figure 6, which showed that the Z direction response was consistently larger in accelerometer #2 than in accelerometer #1 due to the proximity of accelerometer #2 to the path of the wheels.

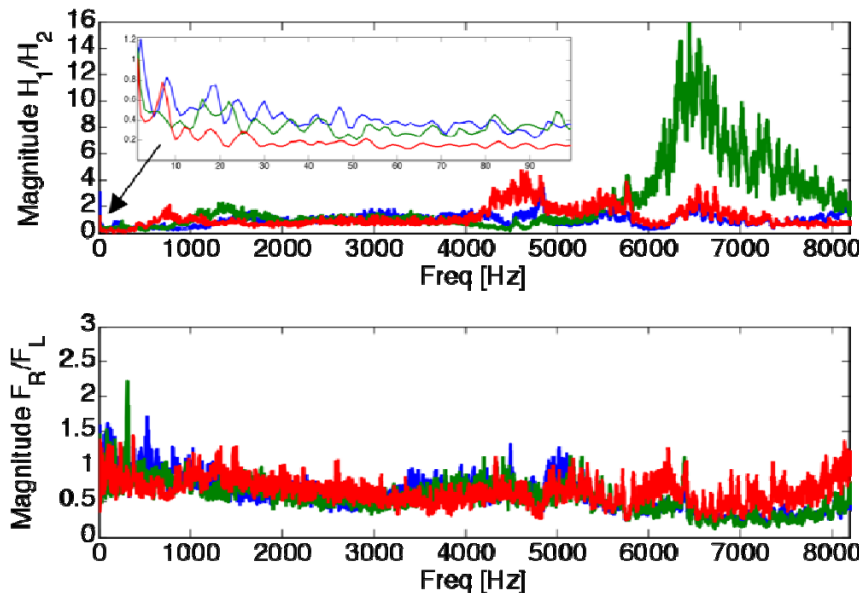


Figure 7: Relationship between (a) frequency response functions and (b) left and right wheel forces for initial baseline (East bound) with three channels of data in (—) X, (—) Y, and (—) Z.

It is also evident that there is amplification of the Y direction response in accelerometer #1 relative to accelerometer #2 in the 1000-2000 Hz range. The spectra shown in Figure 6 are consistent with this finding. It is also interesting to note that the ratios of frequency response functions in the range from 2000-4000 Hz are nearly equal to unity suggesting that in this range the cleat filters the wheel forces similarly in this frequency range. Lastly, note that this frequency response function ratio is primarily a property of the cleat and not a function of the vehicle although there will always be some dependence on the vehicle. The plot in the bottom of Figure 7 indicates that the ratio of the left and right tire forces fluctuates around unity, which would be the expected force ratio in a perfectly symmetric vehicle.

To calculate a fault index, the averaged spectra in the 700-900 Hz range for the ten initial baseline accelerations in the X, Y, and Z directions for accelerometers #1 and #2 as the front wheels traversed the cleat were subtracted from each of thirty comparison datasets as a function of frequency. Then this difference was divided by the standard deviation across the ten initial baseline datasets. Finally, the maximum values of these normalized statistical features were calculated and plotted in Figure 8 for all thirty datasets. It was assumed that a greater than or equal to 2σ variation in this feature would indicate a significant deviation in a dataset due to a fault. The comparison datasets consisted of the ten initial baseline datasets, five additional baseline tests, five right-front suspension fault datasets, five left-rear suspension fault datasets, and five right-front tire pressure fault datasets.

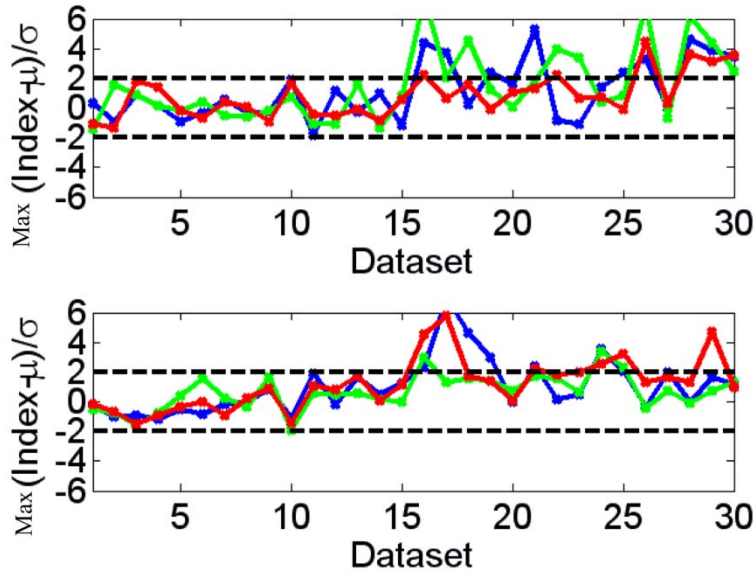


Figure 8: Maximum normalized feature for thirty datasets for accelerometers (a) #1 and (b) #2 for 700-900 Hz frequency range for (—) X, (—) Y, and (—) Z directions for comparison datasets.

The top plot shows the results for accelerometer #1 and the bottom plot shows the results for accelerometer #2. For the first fifteen datasets, which correspond to

the initial and final baseline conditions for which there no tire and suspension subsystem faults, there are no deviations outside $\pm 2\sigma$ (zero false-positives). For the left-front suspension fault, 4 out of 5 faults are detected by the X, Y, and Z directions using accelerometers #1 and #2. For the left-rear suspension fault, 5/5 faults were detected and for the right-front tire fault, 5/5 faults were detected. Based on the features in Figure 8(a), it can be concluded that the tire fault is located in the right-front corner; however, the two suspension faults are not as easy to locate. In future testing, additional baseline and fault datasets will be measured to conduct a more thorough analysis of the ability to locate faults in various corners.

REFERENCES

Thomas, M., "Major Ground Equipment System Accidents Caused by Materiel Failure," 1985, TN 85-3.

DiPetta, T., Koester, D., Adams, D. E., Gotham, J., Decker, P., Lamb, D., and Gorsich, D., "Health Monitoring for Condition-Based Maintenance of a HMMWV using an Instrumented Diagnostic Cleat," 2009, *SAE Congress, Reliability & Robust Design in Automotive Engineering*, in print.